Surfaces and Interfaces 17 (2019) 100360

Contents lists available at ScienceDirect

Surfaces and Interfaces

journal homepage: www.elsevier.com/locate/surfin

Novel pectin from *Parkia biglobosa* pulp mediated green route synthesis of hydroxyapatite nanoparticles

Saheed Ademola Ibraheem[a,*], Ephraim Akuaden Audu[b], Mas'ud Jaafar[a], Judy Atabat Adudu[a], Jeffrey Tsware Barminas[a], Victor Ochigbo[b], Adedoyin Igunnu[c], Silvia Omonirume Malomo[c]

[a] Organic and Natural Products Division, Department of Scientific and Industrial Research, National Research Institute for Chemical Technology, Zaria, Nigeria
[b] Inorganic and Analytical Division, Department of Scientific and Industrial Research, National Research Institute for Chemical Technology, Zaria, Nigeria
[c] Department of Biochemistry, Faculty of Life Sciences, University of Ilorin, Ilorin, Nigeria

ARTICLE INFO

Keywords:
Pectin
hydroxyapatite
nanoparticles
synthesis and *P. biglobosa*

ABSTRACT

Hydroxyapatite (HAP) nanoparticles were synthesized using pectin from pulp of *P. biglobosa* as green template. This was achieved at different concentrations (0.1, 0.5 and 1%) of pectin. The HAP nanoparticles mediated by pectin were characterized using Fourier Transform infrared (FTIR), Scanning electron Microscopy (SEM) and X-ray Diffraction (XRD). Structure and morphology of the synthesized HAP indicate that discrete and less agglomerated particles were produced at low concentration (0.1%) of pectin. The HAP nanoparticles produced, with crystallite size ranging from 17.5 to 26.3 nm, inhibited the growth of selected bacteria used for the study. Findings from this study suggest that *P. biglobosa* pulp pectin can serve as a green template for the production of HAP nanoparticles which are considered to be promising and versatile bioactive materials in enzyme technology, biomedical and tissue engineering.

1. Introduction

Hydroxyapatite (HAP) is an important biologically active material that has been extensively used in regenerative medicine, biomedicine, and dentistry. In terms of chemical composition and its crystal structure, it is similar to apatite, an inorganic constituent of bone and other hard tissues, [1]. HAP possesses excellent binding ability with natural bones and promotes bone growth and integration along its surface [2,3]. Due to its biocompatibility, osteoconductivity and bioactivity; HAP serves an important raw material in bone reconstruction, implants, drug delivery system, scaffolds, cell growth and tissue engineering [4–7].

Hydroxyapartite nanoparticles offer greater advantage over its microstructures due to large surface area to volume ratio. They exhibit distinct improved properties that have attracted the attention of researchers in recent times. They are highly biocompatible and flexible with good bioactivity [8]. They have been found useful in the stimulation of nanostructure growth of inorganic phase in natural hard tissues. They are also involved in controlled release of antigen in vaccines, antibiotics delivery, enzyme technology, anticancer pills and growth factors [9–12]. Synthesis of HAP nanoparticles has been achieved using various methods including microemulsion, hydrothermal, freezing, ultrasonic irradiation, sol-gel precipitation, coprecipitation and chemical templating method. However, these methods are usually complex, labour-intensive, expensive, and potentially hazardous to the environment [13]. In addition, toxic substances used for the synthesis often get adsorbed to the surface of the particles that could have adverse effects in biomedical applications [14]. Consequently, there are renewed efforts by researchers towards synthesis of HAP nanoparticles using environmentally friendly, non-toxic and naturally abundant biomaterials.

Biological materials have been demonstrated to exhibit great potential in the green synthesis of useful and important chemicals including HAP nanoparticles. They are safe, abundant, readily available, totally regenerable, non-exotic, cheap, and able to support rapid growth [15]. *Parkia biglobosa*, known as African locust bean, is an important leguminous tree that is widely distributed across Africa and parts of Southern America and Asia [16]. It is an abundant economic tree in Nigeria that is evenly wide spread across the country [17]. *P. biglobosa* pulp is the yellowish sweet powder that embedded the economic seed, used in the production of locust beans [18]. Despite the nutritional content of the pulp of *P. biglobosa,* it is usually washed away as waste in the processing of the commercially valued locust beans. This does not only lead to environmental pollution (due to improper disposal), it also

* Corresponding author.
E-mail address: saheed.ibraheem@narict.gov.ng (S.A. Ibraheem).

https://doi.org/10.1016/j.surfin.2019.100360
Received 23 May 2019; Received in revised form 13 July 2019; Accepted 21 July 2019
Available online 22 July 2019

constitutes to economic wastes [17].

Different parts of *P. biglobosa* have been reported to exhibit wide range of biological activities including immunomodulating and anti-inflammatory properties [16]. In Africa, they are used in the treatment of ailments such as malaria, ulcer, headache, cough and wound healing [19–21]. Most of these observed effects have been functionally linked to the polysaccharide content of the plant, especially pectin [22].

Pectins are hydrocolloids that are ubiquitously found in cell walls of most higher plants. They are primarily composed of linear chain of poly-α- (1 → 4)-D-galacturonic acid interspersed and branched with units of rhamnose, pentose and hexose [23,24]. As an emerging biomaterial, pectin has the ability to initiate crystal nucleation and growth, therefore invariably enhances bone regeneration. This is achieved by promoting the binding of calcium ion from solution to carboxylate ion [25] due to abundant carboxyl and hydroxyl groups in its structure [26,27].

In recent times, there are reports of green synthesis of HAP nanoparticles using natural sources as templates [12,14,28,29]. To the best of our knowledge, reports on the green synthesis of HAP using abundant and readily available but underutilized pulp of *P. biglobosa* is scarce. In this paper, we present the synthesis of hydroxyapatite nanoparticles using pectin from the pulp of *P. biglobosa* as template. The synthesized hydroxyapatite nanoparticles were characterized using relevant analytical tools and evaluated for antimicrobial properties.

2. Materials and methods

Calcium chloride dihydrate ($CaCl_2.2H_2O$) and ethanol were purchased from BDH Chemicals Ltd Poole, England. Di-ammonium hydrogen phosphate $(NH_4)_2HPO_4$, was a product of Sigma Aldrich, UK. Ammonia was purchased from Prolabo, Normapur. All other chemicals were of analytical grades and used without further purification. Deionized water was used throughout the experimental cycle except where it is stated otherwise.

3. Plant material and pectin extraction

P. biglobosa pods were obtained from the premises of National Research Institute for Chemical Technology, Zaria, Nigeria. The pulp was separated from the seed and pulverized. Pectin extraction was carried out by mixing 100 g of the pulp with 500 ml of HNO_3 acidified water (pH 2). The mixture was boiled for 4 h and filtered using 2-fold muslin cloth and allowed to cool. The pectin was precipitated by mixing 100 ml of the filtrate with 200 ml of absolute ethanol. The precipitated pectin was washed repeatedly with ethyl acetate and ethanol to remove impurities. The residue was then freeze dried, pulverized and kept at room temperature for further use.

4. Synthesis of hydroxyapatite

Typically, pectin (0.02 g) from the pulp of *P. biglobosa* was dissolved in 20 ml water and placed on a magnetic stirrer at 80 °C and 250 rpm for 10 min $CaCl_2.2H_2O$ 0.05 M was added to the solution and stirred for 1 h. Then, 0.03 M $(NH_4)_2HPO_4$ was added in drops for 3 h at 500 rpm. The pH of the mixture was kept constant at 9 by adding aqueous ammonia and stirred for 24 h to obtain a dirty white precipitate. The precipitate was dried in the oven at 80 °C. Ethanol and water were used to wash the dried powder thoroughly to remove residual pectin and chloride ion. The HAP powder was then calcined at 500 °C for 24 h and later sintered at 700 °C for 6 h. These steps were repeated using different concentrations of pectin.

5. Colour test

The colour of the synthesized HAP nanoparticles was evaluated using CIELAB colorimeter, Lovibond PFXi 880/P, Amesbury, UK. a* from green (−) to red (+); b* from blue (−) to yellow (+): L* from black (0) to white (100). The total colour difference (ΔE) was used to determine the colour of the HAP and WI is the whiteness index of the samples [25].

$$\Delta E = \sqrt{(\Delta L^*)^2 + (\Delta a^*)^2 + (\Delta b^*)^2}$$

$$WI = 100 - \sqrt{(100 - L)^2 + a^2 + b^2}$$

Where ΔL*, Δa* and Δb* are the differentials between the colour parameters of the standard (L = 98.87, a = 0.00, b = 0.04) and that of the sample.

Table 1
Colour parameters of *P. biglobosa* pulp pectin mediated hydroxyapatite nanoparticles.

Sample	L*	a*	b*	ΔE	WI
0.1% pectin-HAP	0.14	−1.6	−0.73	98.75	0.12
0.5% pectin-HAP	0.15	0.21	2.31	98.75	0.12
1% pectin-HAP	0.20	2.78	10.36	99.25	−0.38

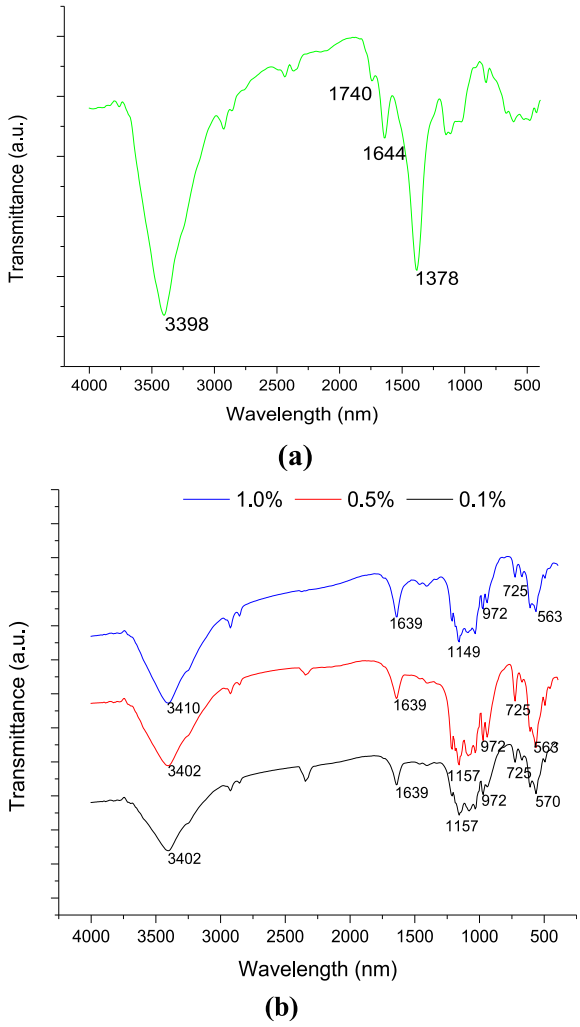

Fig. 1. Fourier Transform spectra of (a) *P. biglobosa* pulp pectin (b) the synthesized HAP nanoparticles.

6. Fourier Transform Infrared (FTIR) spectroscopy

The Fourier Transform Infrared (FTIR) analysis of the samples was done using Shimadzu (FT-IR 8400s, Japan). A small amount of sample

Table 2
Peak attributes of the FTIR bands of synthesized hydroxyapatite nanoparticles.

Sample	OH Stretch	P=O	P-O bending	Degenerate bending P-O	Non-degenerate P-O bending
0.1% pectin-HAP	3402	1149-1041	563	725-671	972-941
0.5% pectin-HAP	3410	1157-1033	563	725-671	972-941
1% pectin-HAP	3402	1157-1041	570	725-671	972-941

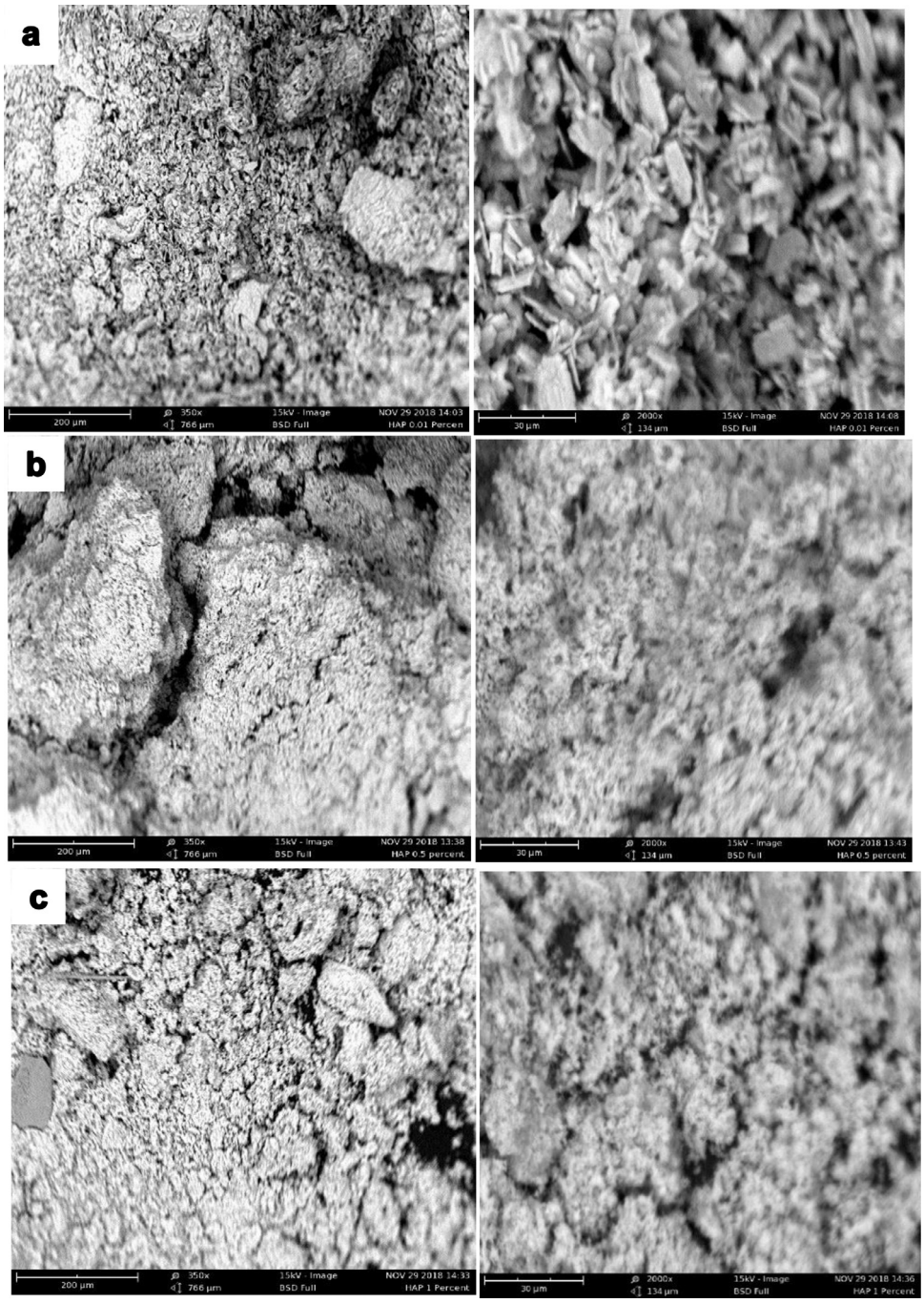

Fig. 2. Scanning electron micrographs of cross section of HAP using (a) 0.1% (b) 0.5% and (c) 1.0% pectin at magnification of ×350 (left) and ×2000 (right).

was blended with KBr and pressed into a pellet prior to analysis. The spectral were collected over the range from 4000 to 400 cm^{-1} with 10 scans and resolution of 2.

7. Scanning Electron Microscopy

The morphology and microstructure of the synthesized HAP nanoparticles were examined using Scanning Electron Microscope (Phenom World X, Netherlands). The samples were mounted on sputter coated gold, standard double faced-holder at the accelerating voltage of 15 kV.

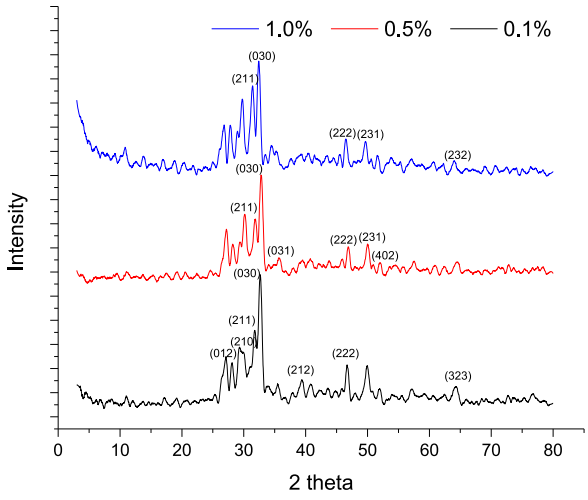

Fig. 3. XRD pattern for the synthesized HAP nanoparticles.

The images were recorded at different magnification from ×350 to ×2000.

8. X-ray diffraction (XRD) analysis

X-ray diffraction (XRD) pattern of the powdered samples were obtained using Rigaku Miniflex 300 (Japan) equipped with Cu-Kα; 1.540598 nm. The scanning was done between 3 and 80 degrees (2θ) at an interval of 0.02 degree per second, 30 kV and 10 mA. The results obtained were collated and analysed using HighScore Plus Software and the spectra matched with the database.

9. Antimicrobial studies

The HAP samples were tested for antimicrobial activity by agar well-diffusion method [30] against Gram positive and negative bacterial strains which include *Staphylococcus aureus, Bacillus subtilis, Pseudomonas aeruginosa* and *Escherichia coli*. The pure cultures of the organisms were sub-cultured on nutrient broth and incubated at 35 °C for 24 h. Sterile nutrient agar was dispensed into the sterile petri dishes and allowed to solidify, after which 5 mm wells were bored on the agar plates using a sterile cork-borer. Aliquots of the organisms in broth (0.1 ml) were evenly spread on each plate using sterile swab sticks. The wells were filled with 100 mg/ml concentration of the HAP at four different volumes (25, 50, 75 and 100 µl) using a sterile micropipette. Ciprofloxacin (5 µg/ml) was used as the control. The Petri-dishes were left for 45 min at room temperature to allow proper diffusion of the extract to occur in the medium and then incubated at 37 °C for 24 h. After incubation, the diameters (mm) of the zones of inhibition were measured.

10. Results and discussion

10.1. Optical properties of the HAP nanoparticles

Table 1 shows the colour parameters of the synthesized HAP nanoparticles using pectin from pulp of *P. biglobosa* as green template. The degree of total colour difference (ΔE) from the standard colour plate did not change when the concentration of pectin was increased from 0.1 to 0.5%. However, there was a slight increase when higher concentration of the pectin (1%) was used for the synthesis. WI, which indicates the degree of whiteness was reduced from 0.12 to −0.38 when the pectin concentration increased from 0.5 to 1%, respectively. ΔE showed the contrast pattern to WI indicating that the colour difference of HAP nanoparticles was due to changes in the whiteness of the samples. These results agree with the visual observations of the synthesized HAP. The finding suggests that high concentration of pectin impacts on the colour of the product formed probably due to impurities which the temperature at which the sample were calcined could not remove. Depending on the area of application, sensory property may play a significant role in the level of success of emerging technologies [25]. HAP nanoparticles have been reported to have wide area of applications including drug delivery, antimicrobial, metal immobilization, coatings and films [31,32]. Therefore, hydroxyapatite synthesized at low pectin concentration can be recommended for use in biomedical sciences.

10.2. FTIR spectrum for pectin

The FTIR spectrum for pectin from the pulp of *P. biglobosa* is shown in Fig. 1a. The broad and intense absorption peak at 3400 cm^{-1} indicates OH stretching vibration of carboxylic acids while C-H stretching of methyl ester of galacturonic acid (the major repeating unit in pectin) can be seen at peak 2800 cm^{-1} [33]. The peak detected at peak 1700 cm^{-1} is assigned to C═O stretching vibration of esterified carboxyl group while peak 1600 cm^{-1} corresponds to C═O stretching vibration of ionic carboxyl group [34]. The peak observed at 1400 cm^{-1} could possibly depict an aromatic or aliphatic C—H vibration of methyl, methylene and methoxy groups. The characteristic peak of C-O-C stretching vibration is found at peak 1238 cm^{-1} which indicate the presence of –O—CH_3 group while the peak found at 955 cm^{-1} corresponds to the presence of glycosides [27]. Pectin contains various functional groups including carboxyl, hydroxyl, ketones and aldehydes [35]. All the above peaks strongly suggest the presence of pectin in the extracted material.

Fig. 1 b shows the FTIR spectra of the synthesized HAP. The major relevant peaks in the spectrum are summarized in Table 2. All the samples exhibit peaks at 3402 and 1643 cm^{-1} which are characteristic of an —OH group stretching and bending vibration respectively. Peaks found between 1200 to 1000 cm^{-1} suggest asymmetric stretching vibration mode (v_3) of phosphate group (P═O) while the peaks at 972 and 941 cm^{-1} were attributed to non-degenerate symmetric stretching modes (v_1) of phosphate group. Characteristic peaks of doubly degenerate bending modes (v_4) of P—O bond are found at 725 and 601 cm^{-1} whereas peak at 563 cm^{-1} suggest a bending mode (v_2) of P—O group. These peaks strongly suggest that the HAP has been synthesized.

The surface and structure micrographs of the synthesized hydroxyapatite at different concentrations of Pectin from *P. biglobosa* are shown in Fig. 2. HAP synthesized with 0.1% pectin seems slightly porous, discrete and flake-like with less degree of agglomeration (Fig. 2a). The particles appear to be non-uniform in terms of shapes and sizes. At 0.5 % pectin, the morphology of the HAP appeared to be spherical and agglomerated compared with HAP synthesized using 0.1 and 1 % pectin (Fig. 2b). This suggests that pectin did not only serves as template for HAP synthesis, it also influences the nature of the particles

Table 3
Structural properties of the synthesized hydroxyapatite powders.

Pectin concentration (%)	Peak position	Plane	FWHM (deg.)	Crystallite size (nm)	Crystallinity (%)
0.1	32.8331	030	0.47232	17.5	0.131
0.5	32.8624	030	0.31488	25.3	0.443
1	32.8331	030	0.47232	17.5	0.131

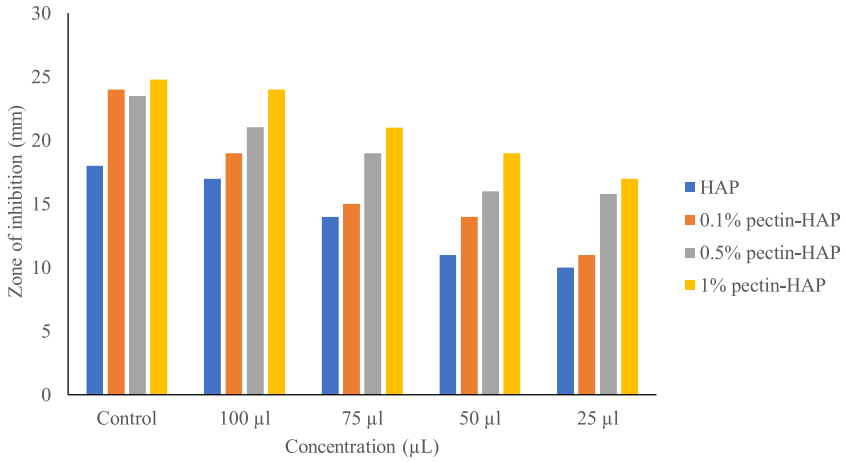

Fig. 4. Zone of inhibition of the sample against *Escherichia coli*.

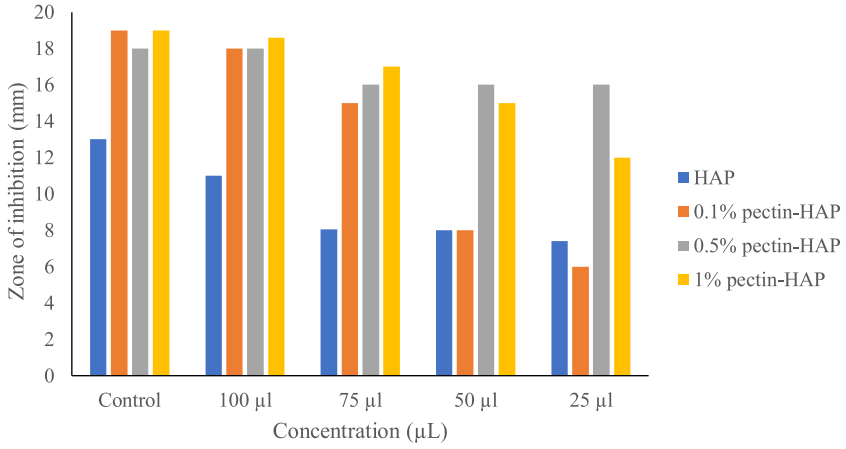

Fig. 5. Zone of inhibition of the sample against *Pseudomonas aeruginosa*.

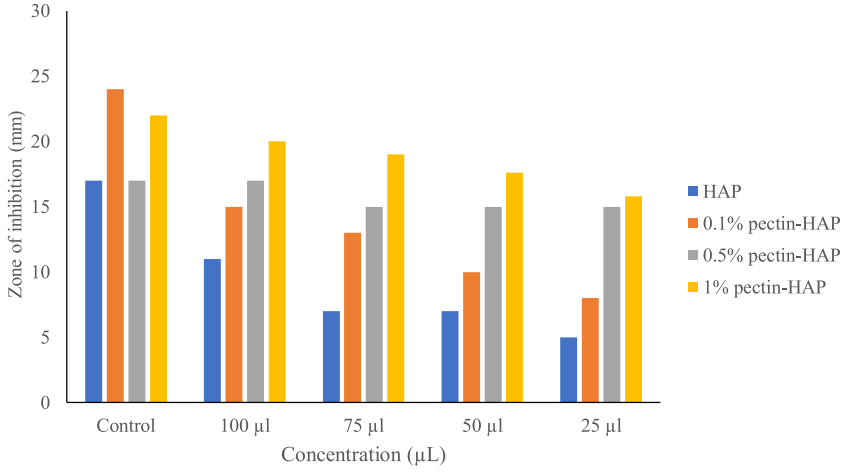

Fig. 6. Zone of inhibition of the sample against *Staphylococcus aureus*.

formed. Polysaccharides have been reported to influence the physical properties of nanomaterials when act as templates [27]

The XRD pattern of the HAP synthesized at different concentrations of pectin from *P. biglobosa* pulp is presented in Fig. 3. At 0.1% pectin template, the diffractions (2θ) at 28.10, 29.32, 31.80, 32.83, 39.47, 46.77 and 64.45 correspond to *h k l* plane of 012, 210, 211, 030, 212, 222 and 323 respectively of HAP (COD file 96-101-1243). The peaks observed at 31.92, 32.86, 35.63, 46.85, 50.16 and 52.06 were matched with planes 211, 030, 031, 222, 231 and 402 respectively at 0.5% pectin. The 1% pectin-template HAP powder produced diffraction peaks at 28.09, 29.32, 31.79, 32.83, 39.46, 46.77 and 64.21. The patterns appear similar and the major characteristic peaks indicate the formation of HAP (COD 96-101-1243). The broadening peaks observed at 32.83 (2θ) with 0.1 and 1% pectin compared to 0.5% indicate decrease in crystallinity and crystallite size. This is supported by the calculated crystallite size and crystallinity according to Scherrer's equation (Table 1). The most intense peak corresponding to plane 030 was used for the determination of the crystallite size and crystallinity of the HAP.

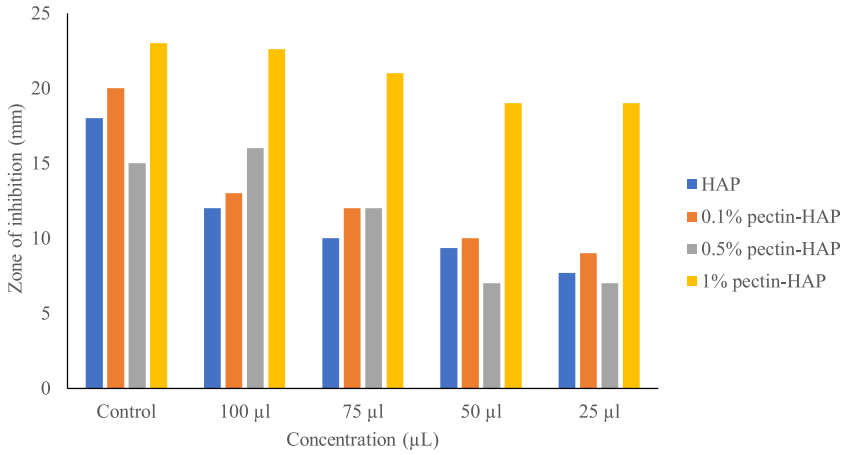

Fig. 7. Zone of inhibition of the sample against *Bacillus subtilis*.

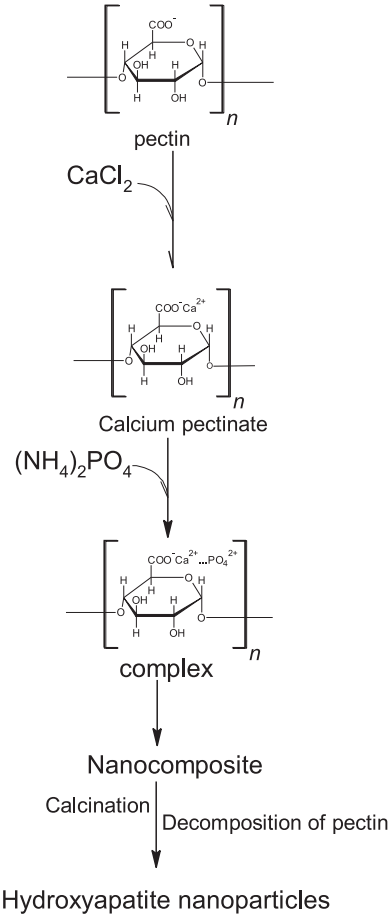

Fig. 8. Possible mechanism of biosynthesis of hydroxyapatite nanoparticles using *P. biglobosa* pulp pectin.

Low crystalline HAP is needed in biomedical sciences because of their high resorbable property *in vivo* [9]. At low concentration of pectin (0.1%), discrete particles of nano HAP with low crystallinity and high purity are produced. This is in agreement with a report that asserted that cross linked pectin molecules provided size effect due to three-dimensional network structure [36] (Table 3).

10.3. Antibacterial activity of the HAP

The antimicrobial activity of HAP synthesized with 0.1g, 0.5g and 1.0g pectin at four different volumes were measured against four bacterial strains. The results are presented in Figs. 4–7. It is apparent that the HAP nanoparticles synthesized in the presence of 1.0 g of pectin showed better antibacterial activity evident from the wide zone of inhibition when compared to HAP synthesized in the absence of pectin. HAP inhibited the growth of *E. coli* with zones of inhibition ranging from 10.00 mm to 24.00 mm. The highest zone of inhibition (24.00 mm) was recorded when the volume of the extract was increased to 100 µl. The control (Ciprofloxacin) had the highest zone of inhibition (24.80 mm) when compared with the highest volume (100 µl) of the nanoparticle.

The zones of inhibition recorded for *P. aeruginosa* ranged from 6.00 mm to 18.60 mm. The zone of inhibition of *P. aeruginosa* recorded by the lowest volume of the sample (25 µl) were 10.00 mm, 11.00 mm, 15.80 mm and 17.00 mm for HAP, 0.1% pectin-HAP, 0.5% pectin-HAP and 1% pectin-HAP respectively. Increasing the volume of sample to 50 µl showed zones of inhibition ranging from 8.00 mm to 16.00 mm for all the samples. On successive increase of the HAP volume to 75 µl and 100 µl, the zones of inhibition ranged from 8.06 mm to 17.00 mm and 11.00 mm to 18.60 mm respectively for HAP, 0.1% pectin-HAP, 0.5% pectin-HAP and 1% pectin-HAP. The inhibition recorded by 100 µl of HAP + 0.5 g Pectin is the same as that of the control (18mm).

For *S. aureus* the zones of inhibition ranged from 5.00 mm to 20.00 mm with the highest inhibition observed in 1% pectin-HAP when the volume was increased to 100 µl. However, the highest inhibition recorded was still lower than the zones of inhibition shown by the control (Ciprofloxacin).

The highest volume of the sample (100 µl) gave the highest zones of inhibition of 12.00 mm, 13.00 mm, 16.00 mm and 22.60 mm for HAP, 0.1% pectin-HAP, 0.5% pectin-HAP and 1% pectin-HAP respectively for *B. subtilis*. The zones of inhibition of the samples were lower when compared with Ciprofloxacin (control).

HAP synthesized with 1.0 g of pectin showed the highest antibacterial activity with zones of inhibition ranging from 12.00 mm to 24.00 mm. Among the four volumes used, 100 µl showed the widest zone of inhibition against *B. subtilis* (22.60 mm), *P. aeruginosa* (18.60 mm), *S. aureus* (20.00 mm) and *E. coli* (24.00 mm), while 25 µl showed the least antibacterial activity with zones of inhibition ranging from 12.00 mm to 19.00 mm. The zones of inhibition are higher than those reported ranging from 5.0 mm to 10.2 mm for *S. aureus* and *E. coli*, respectively using banana peel pectin synthesised hydroxyapatite [27].

Ciprofloxacin (control) showed a higher antibacterial activity against the organisms used in this study. This is may be due to the fact that ciprofloxacin is the most potent fluoroquinolone, active against a broad range of bacteria [37]. The most susceptible being the aerobic Gram-negative *Bacilli*, especially the *Enterobacteriaceae* [38]. It has

often been used as the drug of choice for bacterial infections. The antibacterial activity against *E. coli* was higher than other organisms probably due to the difference in the cell walls between Gram negative (*Pseudomonas aeruginosa* and *Escherichia coli*) and Gram positive (*Bacillus subtilis* and *Staphylococcus aureus*) organisms [27]. Gram negative organisms have a relatively thin cell wall made of peptidoglycans and lipopolysaccharides while Gram positive organisms have a thick cell wall, consisting of a large amount of mucopeptides, murein and lipoteichoic acids [30]. Under certain conditions, the Gram-negative bacteria are more resistant to many chemical agents than Gram-positive cells [39]. Furthermore, the golden carotenoid pigments and the antioxidant enzymes (catalase) of *Bacillus subtilis* give these bacteria a bit stronger oxidant resistance. Also, cell-wall properties, like cell permeability and capability of solubilizing HAP might also be considered [40]. The difference in the antibacterial activity depends on the particles size, nature of the particles, and types of bacteria used for the antibacterial test [41]. The HAP nanoparticles synthesized using pectin as template showed enhanced antibacterial activity against all the organism when compared with the HAP synthesized in the absence of pectin. Remarkably, pectin extracted from various plants have been recorded to possess antibacterial activity due to the presence of some organic components like uronic acid, polyphenols and the presence of minerals such as K^-, Na^+ and Mg^{2+} [27,42-48]. The antibacterial activity of the HAP synthesized with pectin may be due to the presence of these organic compounds and minerals which may be released during the extraction of pectin from *Parkia biglobosa*. Neirynck et al. [49] reported that the presence of elements like K^-, Na^+ and Mg^{2+} are very helpful in improving the biological activities of pectin. The presence of these elements even in trace amounts may play a vital role in enhancing the antibacterial activity of HAP nanoparticles. Presently, many organisms, including bacteria, fungi and plants, have been investigated for the synthesis of metallic nanoparticles and superior antibacterial agents for diagnostic applications. There are several reports on antibacterial properties of nanoparticles [50–54].

10.4. Mechanism of biosynthesis of hydroxyapatite nanoparticles

As shown in Fig. 8, pectic biomolecules possess free reactive carboxylic groups in addition to the esterified carbonyl group. This provides the electrostatic interaction between the carboxyl group (COO^-) and calcium ion introduced in form of calcium chloride [55]. The calcium pectinate complex formed initiates the ionic interaction with phosphate ion (PO_4^{3-}) in order to nucleate the HAP-pectin composite. Subsequently, via calcination process at high temperature, pectin is decomposed and hydroxyapatite formed.

11. Conclusion

This study explores the possibility of using pectin derived from pulp of *P. biglobosa* as green template for the synthesis of hydroxyapatite nanoparticles. Despite the fact that the pulp is abundant, nutritionally rich and contains biologically active components, it is yet to be fully exploited for economic benefits. The synthesized HAP nanoparticles were pure as observed from spectroscopic studies but the size, shape and level of agglomeration depend on the concentration of the pectin used. Reduced size and discrete particle were obtained at 0.1% pectin. This appears to be the optimum concentration of *P. biglobosa* derived pectin template for HAP synthesis. The pulp of *P. biglobosa* seems to be a promising biomaterial for the production of HAP nanoparticles with desired properties for application in tissue engineering.

Acknowledgement

The authors wish to thank Mr Olanipekun Idowu for providing technical assistance while preparing the manuscript.

References

[1] A.A. White, S.M. Best, I.A. Kinloch, Int. J. Appl. Ceram. Technol. 4 (2007) 1–13.
[2] A.B. Rodríguez-Navarro, C. CabraldeMelo, N. Batista, N. Morimoto, P. Alvarez-Lloret, M. Ortega-Huertas, V.M. Fuenzalida, J.I. Arias, J.P. Wiff, J.L. Arias, J. Struct. Biol. 156 (2006) 355–362.
[3] D. Lahiri, S. Ghosh, A. Agarwal, Mater. Sci. Eng. 32 (2012) 1727–1758.
[4] A. Dussan, S. Bertel, S. Melo, F. Mesa, PLoS One 12 (2017) e0173118.
[5] X. Zhang, J. Hui, B. Yang, Y. Yang, D. Fan, M. Liu, L. Tao, Y. Wei, Polym. Chem. 4 (2013) 4120–4125.
[6] J. Hui, X. Zhang, Z. Zhang, S. Wang, L. Tao, Y. Wei, X. Wang, Nanoscale 4 (2012) 6967–6970.
[7] D.S.R. Krishna, A. Siddharthan, S. Seshadri, T.S. Kumar, J. Mater. Sci. Mater. Med. 18 (2007) 1735–1743.
[8] Z. Shi, X. Huang, Y. Cai, R. Tang, D. Yang, Acta Biomater. 5 (2009) 338–345.
[9] S.V. Dorozhkin, M. Epple, Angew. Chem. Int. Ed. 41 (2002) 3130–3146.
[10] M. Roy, S. Nishimoto, Bone 31 (2002) 296–302.
[11] T. Matsumoto, M. Okazaki, M. Inoue, S. Yamaguchi, T. Kusunose, T. Toyonaga, Y. Hamada, J. Takahashi, Biomaterials 25 (2004) 3807–3812.
[12] S.M. Zakaria, S.H. Sharif Zein, M.R. Othman, F. Yang, J.A. Jansen, Tissue Eng. Part B 19 (2013) 431–441.
[13] K.B. Narayanan, N. Sakthivel, Adv. Colloid Interface Sci. 156 (2010) 1–13.
[14] J. Zeng, R. Li, S. Liu, L. Zhang, ACS Appl. Mater. Interf. 3 (2011) 2074–2079.
[15] D. Dhanasekaran, S. Lawanya, S. Saha, N. Thajuddin, A. Panneerselvam, Innov. Roman. Food Biotechnol. 8 (2011) 26.
[16] Y.-F. Zou, B.-Z. Zhang, K.T. Inngjerdingen, H. Barsett, D. Diallo, T.E. Michaelsen, E. Elzoubair, B.S. Paulsen, Carbohydr. Polym. 101 (2014) 457–463.
[17] D.K. De, P. Okonofua, Bagalc J. Pure Apll. Sci. 1 (2001) 40–42.
[18] M.I. Adeniyi, F. Aberuagba, O.D. Adeniyi, AU J. Technol. 14 (2010) 111–118.
[19] O. Chukwu, B. Orhevba, B.I. Mahmood, J. Food Technol. 8 (2010) 99–101.
[20] W. Compaoré, P. Nikièma, H. Bassolé, A. Savadogo, J. Mouecoucou, Curr. Res. J. Biol. Sci. 3 (2011) 64–72.
[21] N.E. Ihegwuagu, M.O. Omojola, M.O. Emeje, O.O. Kunle, Pure Appl. Chem. 81 (2009) 97–104.
[22] K.W. Waldron, C.B. Faulds, Comprehensive Glycoscience, in: H. Kamerling (Ed.), Elsevier, Oxford, 2007, pp. 181–201.
[23] O. Kurita, T. Fujiwara, E. Yamazaki, Carbohydr. Polym. 74 (2008) 725–730.
[24] D. Mudgil, S. Barak, Int. J. Biol. Macromol. 61 (2013) 1–6.
[25] S. Galus, A. Lenart, J. Food Eng. 115 (2013) 459–465.
[26] Y.-C. Wang, Y.-C. Chuang, H.-W. Hsu, Food Chem. 106 (2008) 277–284.
[27] D. Gopi, K. Kanimozhi, N. Bhuvaneshwari, J. Indira, L. Kavitha, Spectrochim. Acta Part A 118 (2014) 589–597.
[28] B. Li, B. Guo, H. Fan, X. Zhang, Appl. Surf. Sci. 255 (2008) 357–360.
[29] D. Gopi, N. Bhuvaneshwari, J. Indira, L. Kavitha, Spectrochim. Acta Part A 104 (2013) 292–299.
[30] H. Ragab, F. Ibrahim, F. Abdallah, A.A. Al-Ghamdi, F. El-Tantawy, N. Radwan, F. Yakuphanoglu, IOSR J. Pharm. Biol. Sci. 9 (2014) 77–85.
[31] J. Li, Y. Chen, Y. Yin, F. Yao, K. Yao, Biomaterials 28 (2007) 781–790.
[32] C.S. Ciobanu, S.L. Iconaru, M.C. Chifiriuc, A. Costescu, P. Le Coustumer, D. Predoi, BioMed Res. Int. 2013 (2013).
[33] Y. Begum, S. Deka, Acta Alimentaria 46 (2017) 428–438.
[34] A. Chatjigakis, C. Pappas, N. Proxenia, O. Kalantzi, P. Rodis, M. Polissiou, Carbohydr. Polym. 37 (1998) 395–408.
[35] N. Yang, W.-H. Li, Ind. Crops Prod. 48 (2013) 81–88.
[36] D. Gopi, K. Kanimozhi, L. Kavitha, Spectrochim. Acta Part A 141 (2015) 135–143.
[37] G. Anquetin, J. Greiner, N. Mahmoudi, M. Santillana-Hayat, R. Gozalbes, K. Farhati, F. Derouin, A. Aubry, E. Cambau, P. Vierling, Eur. J. Med. Chem. 41 (2006) 1478–1493.
[38] P.C. Sharma, A. Jain, S. Jain, R. Pahwa, M.S. Yar, J. Enzyme Inhib. Med. Chem. 25 (2010) 577–589.
[39] G. Tortora, R.B. Funke, L.C. Case, Microbiology: An Introduction, Addison-Wesley Longman, Inc., New York, 2011.
[40] N. Neelakandeswari, G. Sangami, N. Dharmaraj, Synthesis and Reactivity in Inorganic, Metal-Organic, and Nano-Metal Chemistry 41 (2011), pp. 513–516.
[41] G.S. Kumar, S. Rajendran, S. Karthi, R. Govindan, E.K. Girija, G. Karunakaran, D. Kuznetsov, MRS Commun. 7 (2017) 183–188.
[42] I.Y. Bae, Y.N. Joe, H.J. Rha, S. Lee, S.-H. Yoo, H.G. Lee, Food Hydrocolloids. 23 (2009) 1980–1983.
[43] N. Al-Zoreky, Int. J. Food Microbiol. 134 (2009) 244–248.
[44] W.R. Yao, H.Y. Wang, S.T. Wang, S.L. Sun, J. Zhou, Y.Y. Luan, J. Agric. Food Chem. 59 (2011) 5312–5317.
[45] J.-P. Ele-Ekouna, C. Pau-Roblot, B. Courtois, J. Courtois, Carbohydr. Polym. 83 (2011) 1232–1239.
[46] C. Engels, M.G. Gänzle, A. Schieber, Food Res. Int. 45 (2012) 422–426.
[47] L. Fan, M. Cao, S. Gao, W. Wang, K. Peng, C. Tan, F. Wen, S. Tao, W. Xie, Carbohydr. Polym. 88 (2012) 707–712.
[48] M. Jindal, V. Kumar, V. Rana, A. Tiwary, Carbohydr. Polym. 93 (2013) 386–394.
[49] N. Neirynck, P. Van Der Meeren, S.B. Gorbe, S. Dierckx, K. Dewettinck, Food Hydrocolloids. 18 (2004) 949–957.
[50] M. Singh, S. Singh, S. Prasad, I. Gambhir, Digest J. Nanomater. Biostruct. 3 (2008) 115–122.
[51] V. Ravishankar Rai, A. Jamuna Bai, Nanoparticles and Their Potential Application as Antimicrobials, Science against Microbial Pathogens: Communicating Current Research and Technological Advances, in: A. Méndez-Vilas (Ed.), Formatex, Microbiology Series, 1(3) 2011, pp. 197–209.
[52] M. Zargar, A.A. Hamid, F.A. Bakar, M.N. Shamsudin, K. Shameli, F. Jahanshiri, F. Farahani, Molecules 16 (2011) 6667–6676.
[53] M. Taran, M. Rad, M. Alavi, Pharmaceut. Sci. 23 (2017) 198–206.
[54] H.R. Naika, K. Lingaraju, K. Manjunath, D. Kumar, G. Nagaraju, D. Suresh, H. Nagabhushana, J. Taibah Univ. Sci. 9 (2015) 7–12.
[55] F.T. Li, H. Yang, Y. Zhao, R. Xu, Chin. Chem. Lett. 18 (2007) 325–328.